Pathol. Oncol. Res. (2015) 21:405–411
DOI 10.1007/s12253-014-9835-1

RESEARCH

The Apoptotic Effect of Plant Based Nanosilver in Colon Cancer Cells is a p53 Dependent Process Involving ROS and JNK Cascade

Shakti Ranjan Satapathy · Purusottam Mohapatra · Dipon Das · Sumit Siddharth · Chanakya Nath Kundu

Received: 13 May 2014 / Accepted: 13 August 2014 / Published online: 31 October 2014

Abstract Here, we report the p53 dependent mitochondria-mediated apoptotic mechanism of plant derived silver-nanoparticle (PD-AgNPs) in colorectal cancer cells (CRCs). PD-AgNPs was synthesized by reduction of $AgNO_3$ with leaf extract of a medicinal plant periwinkle and characterized. Uptake of PD-AgNPs (ξ, - 2.52±4.31 mV) in HCT116 cells was 3 fold higher in comparison to synthetic AgNPs (ξ, + 2.293±5.1 mV). A dose dependent increase in ROS production, activated JNK and decreased mitochondrial membrane potential (MMP) were noted in HCT116 but not in HCT116 $p53^{-/-}$ cells after PD-AgNP exposure. PD-AgNP-mediated apoptosis in CRCs is a p53 dependent process involving ROS and JNK cascade.

Keywords Silver nanoparticle · Periwinkle · p53 · MAPK · MMP · ROS · Colon cancer

Introduction

Recently, we have shown that starch coated AgNPs (ξ, +2.293± 5.1 mV) caused colon cancer cell death by induction of apoptotic markers BAX/BCL-XL, caspases (3, 8 and 9), cleaved product PARP, p53 and DNA damage [1]. Using isogenic HCT116 and HCT116 $p53^{-/-}$ cell lines, we have also shown that tumor suppressor p53 is the central protein for causing the apoptosis. But the detail p53 dependent mitochondria-mediated cell damage remained unknown. Synthetic AgNP is an inappropriate model to study the biochemical action due to its multiple limitations that include effectiveness at higher doses; synthesis involves a mixture of several biological hazardous materials, may provide erroneous conclusion [2, 3]. Thus, nonhazardous, environmentally safe, nontoxic-substance mediated green or biogenic nanoparticle is the better model compared to its synthetic counterpart [4].

Synthesis of biogenic nanoparticle has been reported from yeast [5], fungi [6], bacteria [5], and plant extracts [7]. But nanoparticle synthesis using plant extracts is simplest as compared to microbes based methods [5–7]. Reports exist regarding the plant based synthesis of silver (Ag) and gold (Au) nanoparticles [8, 9]. *Catharanthus roseus* (Periwinkle) is a medicinal plant well-known for its anti-bacterial [10], anti-diabetic [11], anti-plasmodial [12], and anti-cancer properties [13]. Synthesis of AgNP using periwinkle leaf extract as a reducing and capping agent has also been reported [12].

In the current study, we have investigated p53 dependent mitochondria-mediated anticancer activity of plant based nanosilver (PD-AgNPs) in colon cancer cells. PD-AgNPs are more active than synthetic AgNPs and displayed higher anti-cancer potentiality at significantly lower doses. Their anti-cancer activity involved activation of JNK cascade, increased Cytochrome C release, ROS production and reduction in the mitochondrial membrane potential. These activities are largely p53 dependent.

Materials and Methods

Cell Culture and Chemicals

Human colon carcinoma cells HCT116 and HCT116 $p53^{-/-}$ were grown according to protocol described earlier [1]. In

Electronic supplementary material The online version of this article (doi:10.1007/s12253-014-9835-1) contains supplementary material, which is available to authorized users.

S. R. Satapathy · P. Mohapatra · D. Das · S. Siddharth · C. N. Kundu (✉)
Cancer Biology Division, KIIT School of Biotechnology, KIIT University, Campus-11, Patia, Bhubaneswar, Orissa 751024, India
e-mail: cnkundu@gmail.com

brief, cells were cultured in DMEM with 1 % antibiotic (penicillin and streptomycin) and 10 % FBS in 5 % CO_2 at 37 °C. Cell culture materials, fine chemicals and antibodies were purchased from HiMedia® Ltd (Mumbai, India), Sigma Chemical Ltd. (St. Louis, MO, USA) and Cell Signaling Technology (MA, USA), respectively.

Synthesis of Plant Derived AgNPs (PD-AgNPs)

Freshly collected *C.roseus* leaves were shredded to small pieces, shade dried and powdered. 5 gm of the leaf powder was boiled for 15 min in 100 mL sterile water and then cooled followed by sequential filtration through 0.2 μm filter. 10 mL of extract was added into 90 mL of 1 mM $AgNO_3$ for reduction to Ag^+ ions and incubated overnight at RT in dark with constant stirring [13]. The purple yellow color and characteristic peak at 420 nm confirms silver nanoparticle and designated as PD-AgNPs [1]. The physiochemical property of PD-AgNPs showed a 20 nm spherical shape having a negative zeta potential (−2.52±4.31 mV) (data not shown). Detail preparation and characterization of synthetic AgNP has been provided earlier [1].

Cell Viability Assay

To test the effect of PD-AgNPs, $AgNO_3$, leaf extract and starch embedded synthetic AgNPs on growth of cells, an MTT assay was carried out as described earlier [1]. Briefly, 8,000-10,000 cells/well were seeded in a 96 well tissue culture plate for 24 h then were exposed to the agents for 48 h. Then MTT reagent was added and OD was measured at 570 nm after dissolving the purple crystals with detergent. Experiment was repeated atleast thrice.

Clonogenic Cell Survival Assay

Clonogenic assay was performed to measure the effect of PD-AgNP in cell survival as described earlier [1]. Cells (800–1,000 cells/well) were seeded for 24 h, and then exposed to PD-AgNPs as indicated for 48 h. The media was replaced in every 2 days with fresh medium and cells were allowed to grow for 5–6 doublings. After staining with crystal violet, the colonies were counted using a Gel documentation system (UVP, CA, USA). Assay was performed at least thrice.

FACS Analysis

Cell cycle profile and apoptosis was analyzed by FACS to test the effect of PD-AgNPs on HCT116 cells according to protocol described earlier [1]. Briefly, cells were exposed to PD-AgNPs for 48 h. Then were fixed with 70 % ethanol and kept at −20 °C overnight and followed by staining with 0.1 mL of 50 μg/ml Propidium Iodide (PI). Cells were sorted using FACS (FACS Calibur, Becton and Dickinson, CA, USA) and 10,000 events were captured. Different phases of the cell cycle were determined using Cell Quest Pro Software (Becton and Dickinson, CA, USA).

Cellular Uptake Study by FACS

Cellular uptake efficiency of PD-AgNPs was measured by FACS using an earlier report with little modification [14]. Briefly, (1×10^5) cells/well were grown and exposed to PD-AgNPs and synthetic AgNPs for 5 h. Cells were washed with 1X PBS to remove the unbound NPs and the amount of NP uptake was analyzed by FACS (FACS Canto II, Becton and Dickinson, CA, USA) and 10,000 events were captured. Pacific blue filter was used to capture the excitation of AgNPs [15]. The increase of fluorescence in the NP treated cells relative to that of untreated control cells was expressed as mean fluorescence intensity (MFI).

Mitochondrial Membrane Potential (MMP) Analysis

MMP was analyzed by FACS using MitoTracker Red (Cat# M-7512, Invitrogen, CA, USA) [16]. MitoTracker red is a cationic fluorescent dye that can easily be taken up by the active mitochondria due to highly negative MMP ($\Delta\psi_m$). Intensity of the fluorescent signal obtained is an indicator of MMP. Depolarization of $\Delta\psi_m$ results the loss of MitoTracker Red and a decrease in the fluorescence intensity indicated by peak shift from right to left.

For this study, 1.5×10^5 cells/well were seeded in 6-well plates and were exposed to PD-AgNPs for 48 h. Then cells were washed with 1X PBS and incubated with MitoTracker red at 37 °C for 30 min in the dark. Cells were again washed twice with 1X PBS and fluorescence was measured by FACS at 579 nm.

Analysis of ROS Generation

ROS generation in cells was analyzed with the 2′, 7′-dichlorofluorescin diacetate (DCFH-DA) [17]. Briefly, 1×10^5 cells were plated in 6-well plate and were exposed to PD-AgNPs for 48 h, then stained with DCFH-DA for 15 min at 37 °C in the dark. Then it was washed twice with 1X PBS and analyzed with FACS.

Western Blotting

1×10^6 cells/100 mm dishes were plated and were exposed to PD-AgNPs for 48 h. Then whole cell lysates were made and processed for western blot analysis according to antibody manufacturing protocol.

Statistical Analysis

A two-tailed Student's *t*-test was used, where $p<0.05$ was considered to be statistically significant.

Results

PD-AgNP Caused Apoptosis in Colon Cancer Cells

MTT cell viability assay was carried out to determine the anti-proliferative activity of PD-AgNPs on colon cancer cells. Fig. 1a demonstrates the dose dependent reduction of HCT116 cell growth after 48 h PD-AgNP treatment with a LC_{50} of 450 nM. Synthetic AgNPs and $AgNO_3$ although induced cell death but the extent of cell killing ability was less as compared to PD-AgNPs (Fig. 1a). $AgNO_3$ or synthetic AgNPs failed to elicit LC_{50} even at 10 μM. It is interesting to note that there was no significant decrease of cell viability observed in presence of plant extract alone (Fig. 1a). LC_{50} value at different time interval was recorded as 270 nM, 450 nM and 540 nM at 72, 48 and 24 h, respectively in PD-AgNP treated HCT116 cells (data not shown).

Next, we investigated the effects of p53 on PD-AgNP-mediated cell death, in HCT116 and HCT116 $p53^{-/-}$ cell lines. Both the cell lines were treated with PD-AgNPs (0–750 nM) for 48 h and it was observed that *p53* null cells were more resistant to PD-AgNPs; induce cell death of 20 % at 1 μM (Fig. 1b). Effect of PD-AgNPs on clonogenicity was tested. A significant reduction of colony formation was noted in HCT116 cells treated with LC_{50} concentration (450 nM) of PD-AgNPs. In contrast, no appreciable reduction in colony formation was observed in HCT116 $p53^{-/-}$ cells up to 1 μM (Fig. 1c).

FACS analysis and DAPI nuclear staining (data not shown) was performed to confirm the PD-AgNP mediated apoptosis and regulation of cell cycle in HCT116 cells. Fig. 1d showed an increase in apoptotic population with increasing concentrations of PD-AgNPs. More than 40 and 78 % cells were accumulated in Sub-G_1 phase at 450 nM and 750 nM of PD-AgNPs exposure, respectively (Fig. 1d). Interestingly, it was noted that the G_1 and G_2/M phase population decreased with increasing concentrations of PD-AgNPs. Thus, data indicates PD-AgNPs are more effective in inducing cell death as compared to synthetic AgNPs and PD-AgNP mediated cell death is p53 dependent.

Accumulation of PD-AgNPs in Cells

The higher cell killing ability of PD-AgNP is may be due to the enhanced accumulation of NP inside the cells as compared to synthetic AgNP at a fixed dose. To check this possibility, the cellular uptake of PD-AgNPs and synthetic AgNPs was measured by FACS (Fig. 2a). A relative increase of MFI was noted after dose dependent treatment of NPs. However, the accumulation of PD-AgNPs was higher in comparison to synthetic NPs at same dose. The MFI for the PD-AgNPs and synthetic AgNPs were 93.5 and 33.6, respectively at 450 nM (Fig. 2a). The cellular uptake of PD-AgNPs is ~3 times higher than that of synthetic counterpart at 450 nM (Fig. 2a). It is interesting to note that there was no significant difference of NP accumulation observed in PD-AgNP treated HCT116 and HCT116 $p53^{-/-}$ cells (data not shown).

PD-AgNP Induced ROS by Reduction of MMP

MMP was measured to determine the mitochondrial membrane integrity after NP treatment. The MMP was decreased with increasing dose of PD-AgNPs (0–750 nM) with a shift in peak from right to left. More than 6 fold reduction of MMP was noted in HCT116 cells at 750 nM PD-AgNP in comparison to untreated cells (Fig. 2b). Interestingly, no significant change in MMP was noted in HCT116 $p53^{-/-}$ cells after same dose of PD-AgNP treatment (Fig. 2c).

The reduction of MMP indicates the involvement of oxidative stress and increase in ROS. A significant increase in relative intracellular ROS level was observed with increasing dose of PD-AgNPs. At 750 nM PD-AgNP treated cells showed 10 % higher ROS generation in comparison to untreated cells (Fig. 2d). ROS production in HCT116 $p53^{-/-}$ was negligible (1.2 %) even at higher doses (750 nM). Hydrogen peroxide (H_2O_2) treated (positive control) cells showed a significant increase (~20 %) in ROS levels as compared to untreated controls. Data suggest PD-AgNP mediated apoptosis involves loss in MMP with ROS generation and is p53 dependent.

PD-AgNPs Induces Apoptosis Through a p53 Dependent MAPK Cascade

Expression levels of representative pro-apoptotic and anti-apoptotic markers including BAX/BCL-XL ratio, PARP, p53 along with the p-p53 were checked by western blot analysis in the PD-AgNPs exposed cells. Expression of BCL-XL was reduced with concomitant increase in BAX and 3 fold increase in cleaved PARP (89 kDa), 9 fold increase in p-p53 (Ser 15) and 5 fold increase in p53 as well as 7 fold increase in caspases 3 levels with increasing doses of PD-AgNPs treated HCT116 cells as compared to untreated control (Fig. 3a). Interestingly, no significant changes were noted in expression levels of any of these proteins in PD-AgNP exposed HCT116 $p53^{-/-}$ cells (Fig. 3a).

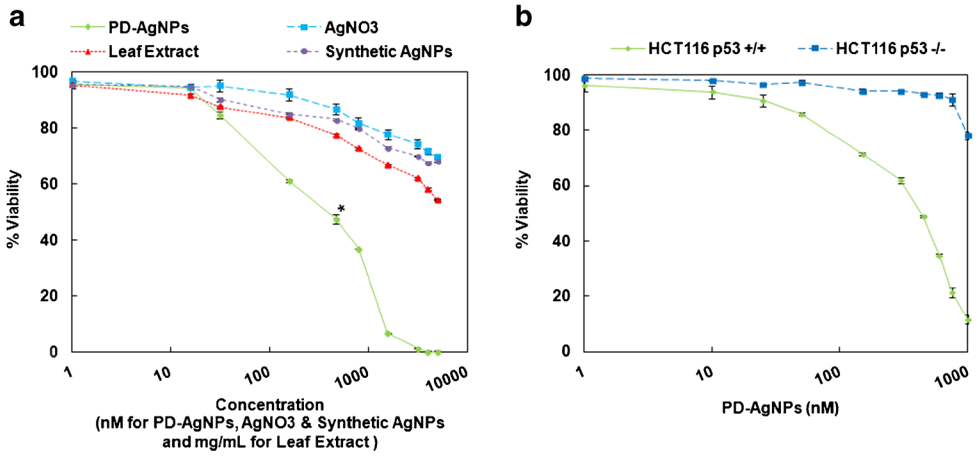

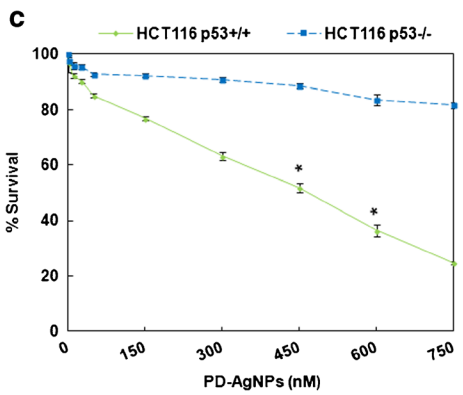

d

PD-AgNPs (nM)	Sub-G1	G1	S	G2/M
0	3.23 ± 0.5	45.91 ± 0.7	22.15 ± 0.2	15.36 ± 0.6
50	3.41 ± 0.6	15.14 ± 0.5	38.80 ± 0.9	12.22 ± 0.4
150	5.29 ± 0.9	2.14 ± 0.4*	45.05 ± 0.9*	4.11 ± 0.2
450	40.67 ± 2.2*	3.35 ± 0.8	4.81 ± 0.8	3.94 ± 0.2*
750	78.87 ± 5.8	3.48 ± 0.9	2.31 ± 0. 3	0.50 ± 0.1*

Fig. 1 PD-AgNP caused apoptosis in HCT116 cells. PD-AgNPs reduced the anchorage dependent cell growth. Cells were exposed to increasing concentrations of leaf extract, $AgNO_3$, synthetic AgNPs and PD-AgNPs then MTT cell viability assay was carried out. **(a)** The semi-log graph of percent viability (Y-axis) vs. concentrations (X-axis). (**b & c**) Cytotoxicity of PD-AgNPs is p53 dependent: HCT116 $p53^{+/+}$ and HCT116 $p53^{-/-}$ cell lines were exposed to PD-AgNPs then cell viability and clonogenic assay were carried out**. (b)** MTT Assay. The semi-log graph was plotted with percent viability (Y-axis) vs. concentrations (X-axis). **(c)** Clonogenic assay. The graph plotted with percent survival (Y-axis) vs. concentrations (X-axis). **(d)** FACS analysis of PD-AgNPs treated cells. HCT116 cells were treated with PD-AgNPs and subjected to FACS analysis. Data was the mean±SD of 3 independent experiments. Statistical significance was determined by paired *t* test. *$p<0.05$

Earlier reports suggest that p53 mediates MAPK dependent apoptosis in cancer cells [18–20]. To check whether AgNP-induced p53 regulates apoptosis by modulating the MAPK signaling cascade, we have measured the major intermediates of MAPK cascade (e.g. JNK and p-JNK, c-JUN) in PD-AgNPs treated cells. Interestingly, a 4 fold, 5 fold and 7 fold increase in the expression levels of JNK, c-JUN and phosphorylated JNK (p-JNK-Thr183/Tyr185) proteins, respectively were noted in treated cells (750 nM) as compared to untreated cells. But the levels of p38, phospho-p38 (Thr180/Tyr182) and ERK, phospho-ERK (Thr202/Tyr204) did not show any appreciable alteration (Fig. 3b). Thus data implies that MAPK cascade is involved in PD-AgNP mediated apoptosis. To confirm p53-dependence and MAPK involvement in this process a similar experiment was carried out in HCT116 $p53^{-/-}$ cells. The levels of JNK, p-JNK (Thr183/Tyr185), p38, p-p38 (Thr180/Tyr182), ERK, p-ERK (Thr202/Tyr204) and c-JUN remained unaffected with PD-AgNPs treatment, hence clearly indicating involvement of p53 and MAPK signaling in PD-AgNP mediated apoptosis (Fig. 3b).

Discussion

Using colon cancer cell lines, we have recently shown that chemically synthesized silver-based nanoparticles (AgNPs) effectively kill the colon cancer cells by multiple targets [1]. Here, using the same model (human colon cancer cells, isogenic HCT116 and HCT116 $p53^{-/-}$) and plant derived AgNPs (PD-AgNPs), we have studied detailed action of p53 dependent mitochondria-mediated cell death phenomenon in cells. PD-AgNPs were synthesized by an easy single step procedure that involves addition of aqueous solutions of periwinkle leaf extract and $AgNO_3$ at RT. There is no involvement of any harmful solvent, toxic chemical, complex step for the synthesis; moreover, this procedure is eco-friendly and economical. Physiochemical properties of nanosilver were measured by multiple assays for confirmation and characterization. Interestingly, it was noted that periwinkle leaf extract (*C.roseus*) did not show any significant cell killing property in cells unlike the nanoparticles (Fig. 1a). PD-AgNPs showed significantly enhanced activity as compared to the synthetic AgNPs,

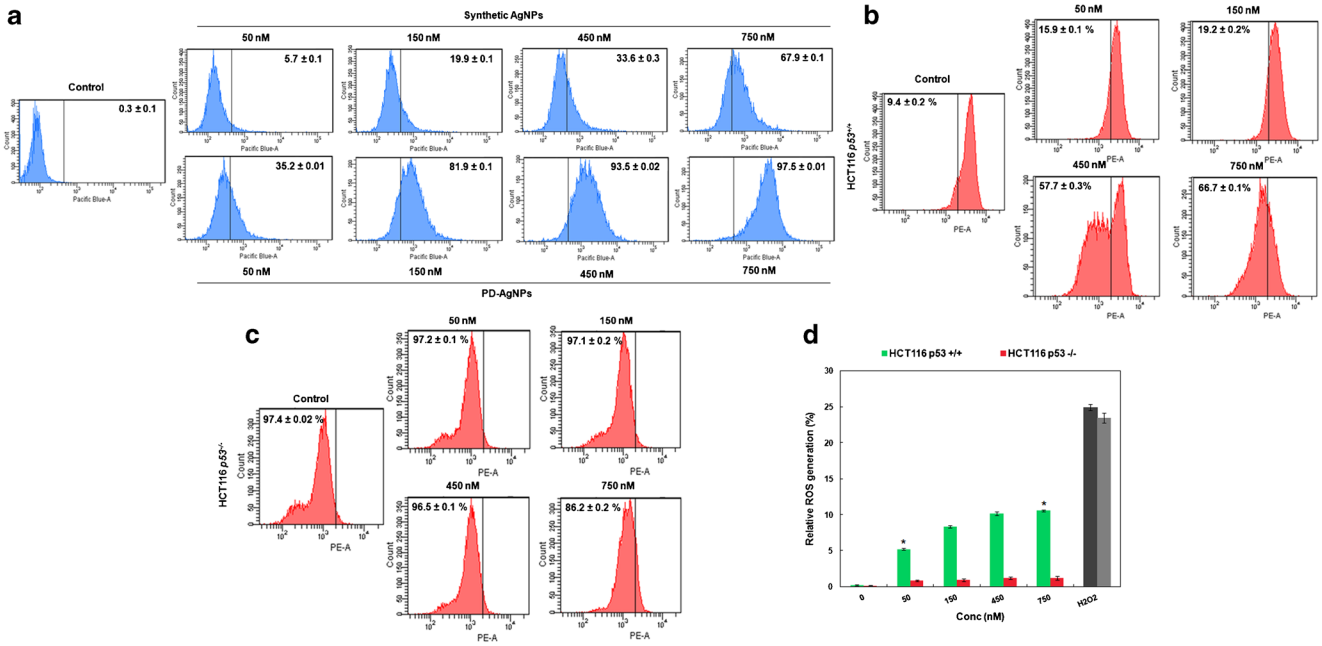

Fig. 2 PD-AgNP increased ROS formation and reduced mitochondrial membrane potential (MMP). (**a**) Cellular uptake of silver nanoparticle measured by FACS. HCT116 cells were exposed to NPs and then uptake was measured. Images were shown average MFI of NPs. (**b, c**) MMP and (**d**) ROS measurement. The PD-AgNP exposed cells were incubated with MitoTracker and DCF-DA dye for the measurement of MMP (**b & c**) and ROS (**d**), respectively using FACS. (**b**) HCT116 cells and (**c**) HCT116 $p53^{-/-}$ cells. (**d**) ROS production. Graph representing the relative ROS production in Y-axis and PD-AgNPs (nM) in X axis. H_2O_2 treated cells were used as positive control. Data shown was the mean±S.D. of 3 different experiments. Statistical significance was determined by paired *t* test. $^*p<0.05$

as it induced higher apoptotic activity in HCT116 cells at comparatively lower concentrations than the synthetic AgNPs (LC_{50} for PD-AgNPs is 450 nM Vs 100 μM for synthetic AgNPs [1]. Interestingly, it was noted that at similar culture conditions cellular uptake of plant derived AgNPs was more in comparison to chemically derived AgNPs (Fig. 2a). Like synthetic AgNPs, PD-AgNPs caused apoptosis through induction of p53, PARP cleavage and BAX/BCL-XL ratio.

Next, we examined the mechanism of huge increase of cell killing activity (approx. 220 fold) of PD-AgNPs compared to AgNP. TEM and DLS analysis revealed the spherical shape of PD-AgNPs with 20 nm (data not shown). A significant difference in ξ, between PD-AgNPs and synthetic AgNPs was noted; PD-AgNPs possess negative ξ, (−2.52±4.31 mV) in contrast to positive ξ, of synthetic AgNPs (2.293±5.1 mV) (data not shown) [1]. Multiple reports suggest that negative ξ, facilitates easy penetration of the particle into the cells. Electrostatic interactions of NPs with the positively charged cell surface receptors or nuclear import factors, lead to localized neutralization and a subsequent bending of the membrane favoring endocytosis, resulting in easy penetration into the cell [21–23]. PD-AgNPs with a negative ξ, leads to higher cellular uptake and enhanced apoptosis at very low nM concentrations. However, further investigation is needed to understand the mechanism for their efficient cellular uptake. No difference of uptake of NP but significant increase of cell death in HCT116 (LC_{50} 450 nM) in comparison to HCT116 $p53^{-/-}$ (LC_{50} 1 μM) confirm the contribution of p53 in NP mediated cytotoxicity.

MMP ($\Delta\psi_m$) controls ATP synthesis, proteins import into the mitochondrion and membrane potential dynamics in cells. Report also suggests that nanoparticles induced oxidative stress in mitochondria and caused low ATP yield [3, 24, 25]. PD-AgNPs treated cells showed increase ROS production indicating the influence of nanoparticles on respiratory chain. Under stress, the mitochondrial membrane pores open and $\Delta\psi_m$ disrupt as a result Cytochrome C release to the cytosol and cause apoptosis [16, 26–28]. BCL-XL prevents the opening of pore [27], while BAX accelerates the phenomena. The increased BAX/BCL-XL ratio, ROS production and decreased MMP as well as increased Cytochrome C expression in HCT116 cells but unalteration in HCT116 $p53^{-/-}$ cells suggest the PD-AgNP mediated apoptosis involved mitochondrial damage and dependent on p53.

Mitogen Activated Protein Kinases (MAPK) is one of the major pro-apoptotic signaling cascade activated upon various external and internal stimuli [29]. Tumor suppressor p53 and MAPK signaling coordinately regulate the cell death pathways in various cell lines [18–20]. Reports suggest that, AgNPs caused apoptosis in NIH3T3 and HCT116 cells by activating MAPK signaling cascade [30]. Interestingly, we observed that JNK, p-JNK and c-JUN were significantly altered without affecting the levels of p38, p-p38 and ERK,

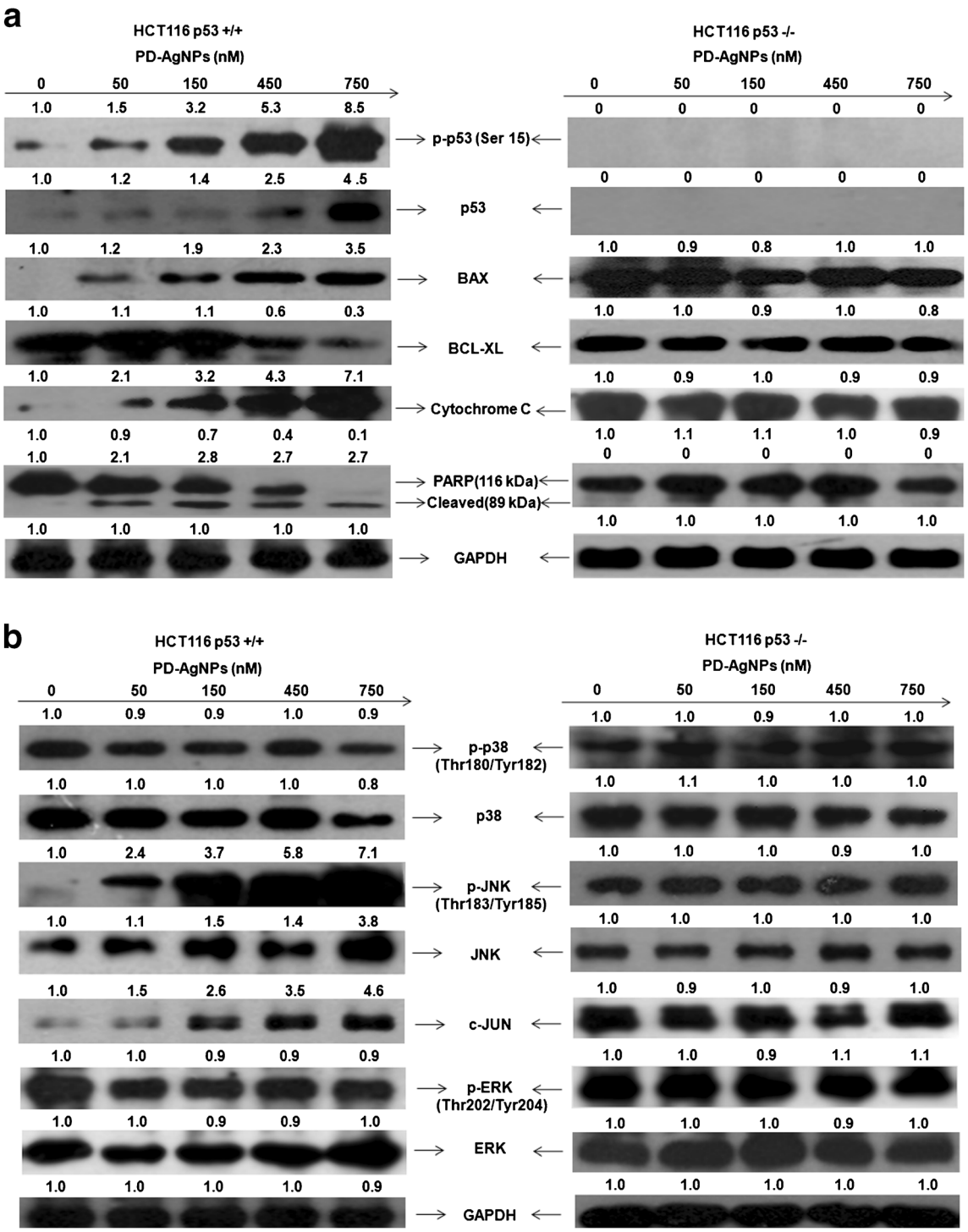

Fig. 3 PD-AgNPs caused apoptosis by p53 mediated MAPK signaling cascade. HCT116 and HCT116 $p53^{-/-}$ cells were treated with PD-AgNPs. Whole cell lysates were prepared and western blot was performed with respective antibody as indicated. (**a**) Expressions of representative pro-apoptotic, anti-apoptotic proteins. (**b**) Expressions of components of MAPK signalling cascade. GAPDH served as loading control. The numerical values indicated upper of each panel represent the relative fold change of protein expression with respect to control by densitometry

p-ERK in HCT116 cells but not noted in HCT116 $p53^{-/-}$ cells after PD-AgNP treatment (Fig. 3). But detail study need to be carried out for understanding the contribution of AgNP-mediated p53 activation in relation to ROS production and subsequent apoptotic process. This is the first report showing the direct linkage between MAPK signaling and mitochondrial mediated cancer cell death involving p53. Thus, the status of p53 will be the marker for action of PD-AgNP mediated

apoptosis in colon cancer cells. To conclude further more study will be needed in animal and human patient sample.

In conclusion, the present report reveals that PD-AgNPs caused apoptosis by induction of ROS, reduction of MMP and increased the expression of major components of MAPK signaling cascade particularly JNK pathway. Finally, this apoptotic activity is p53 dependent.

Acknowledgments Authors are greatly acknowledged Prof. Bert Vogelstein, Johns Hopkins, Baltimore, USA for providing HCT116 $p53^{-/-}$ cell lines and also thanks to ICMR and DBT, Govt. of India for financial support.

Conflict of Interest The authors declare no conflict of interest.

References

1. Satapathy SR, Mohapatra PM, Preet R, Das D, Sarkar B, Choudhuri T, Wyatt MD, Kundu CN (2013) Silver nanoparticles induce apoptosis in human colon cancer cells mediated through p53. Nanomedicine 8:1307–1322. doi:10.2217/nnm.12.176
2. Tao A, Sinsermsuksaku P, Yang P (2006) Polyhedral silver nanocrystals with distinct scattering signatures. Angew Chem Int Ed 45:4561–4597. doi:10.1002/anie.200601277
3. AshaRani PV, Low Kah Mun G, Hande MP, Valiyaveettil S (2009) Cytotoxicity and genotoxicity of silver nanoparticles in human cells. ACS Nano 3:279–290. doi:10.1021/nn800596w
4. Raveendran P, Fu J, Wallen SL (2003) Completely "green" synthesis and stabilization of metal nanoparticles. J Am Chem Soc 125:13940–13951. doi:10.1021/ja029267j
5. Jha AK, Prasad K, Kulkarni AR (2009) Synthesis of TiO_2 nanoparticles using microorganisms. Colloids Surf B: Biointerfaces 71:226–229. doi:10.1016/j.colsurfb.2009.02.007
6. Dhillon GS, Brar SK, Kaur S, Verma M (2012) Green approach for nanoparticle biosynthesis by fungi: current trends and applications. Crit Rev Biotechnol 32:49–73. doi:10.3109/07388551.2010.550568
7. Iravani S (2011) Green synthesis of metal nanoparticles using plants. Green Chem 13:2638–2650. doi:10.1039/C1GC15386B
8. Mukunthan K, Balaji S (2012) Cashew apple juice (Anacardium occidentale L.) speeds up the synthesis of silver nanoparticles. Int J Green Nanotechnol 4:71–79. doi:10.1080/19430892.2012.676900
9. Kasthuri J, Veerapandian S, Rajendran N (2009) Biological synthesis of silver and gold nanoparticles using apiin as reducing agent. Colloids Surf B: Biointerfaces 68:55–60. doi:10.1016/j,colsurfb.2008.09.021
10. Goyal P (2008) In vitro evaluation of crude extracts of Catharanthus roseus for potential antibacterial activity. Int J Green Pharm 2:176–181. doi:10.4103/0973-8258.42739
11. Rasineni K, Bellamkonda R, Singareddy SR, Desireddy S (2010) Antihyperglycemic activity of *Catharanthus roseus* leaf powder in streptozotocin-induced diabetic rats. Pharmacogn Res 2:195–201. doi:10.4103/0974-8490.65523
12. Ponarulselvam S, Panneerselvam C, Murugan K, Aarthi N, Kalimuthu K, Thangamani S (2012) Synthesis of silver nanoparticles using leaves of Catharanthus roseus Linn. G. Don and their antiplasmodial activities. Asian Pac J Trop Biomed 2:574–580. doi:10.1016/S2221-1691(12)60100-2
13. Jacob SJ, Finub JS, Narayanan A (2012) Synthesis of silver nanoparticles using Piper longum leaf extracts and its cytotoxic activity against Hep-2 cell line. Colloids Surf B: Biointerfaces 91:212–214. doi:10.1016/j.colsurfb.2011.11.001
14. Suzuki H, Toyooka T, Ibuki Y (2007) Simple and easy method to evaluate uptake potential of nanoparticles in mammalian cells using a flow cytometric light scatter analysis. Environ Sci Technol 41:3018–24. doi:10.1021/es0625632
15. Parang Z, Keshavarz A, Farahi S, Elahi SM, Ghoranneviss M, Parhoodeh S (2012) Fluorescence emission spectra of silver and silver/cobalt nanoparticles. Scientia Iranica F 19:943–47. doi:10.1016/j.scient.2012.02.026
16. Chairuangkitti P, Lawanprasert S, Roytrakul S, Aueviriyavit S, Phummiratch D, Kulthong K, Chanvorachote P, Maniratanachote R (2013) Silver nanoparticles induce toxicity in A549 cells via ROS-dependent and ROS-independent pathways. Toxicol Vitro 27:330–338. doi:10.1016/j.tiv.2012.08.021
17. Kumar S, Sitasawad SL (2009) N-acetylcysteine prevents glucose/glucose oxidase-induced oxidative stress, mitochondrial damage and apoptosis in h9c2 cells. Life Sci 84:328–36. doi:10.1002/jctb.2023
18. Wu GS (2004) The functional interactions between the p53 and MAPK signaling pathways. Cancer Biol Ther 3:156–161. doi:10.4161/cbt.3.2.614
19. Saha MN, Jiang H, Yang Y, Zhu X, Wang X, Schimmer AD, Qiu L, Chang H (2012) Targeting p53 via JNK Pathway: a novel role of RITA for apoptotic signaling in multiple myeloma. PLoS ONE 7: e30215. doi:10.1371/journal.pone.0030215
20. Taylor CA, Zheng Q, Liu Z, Thompson JE (2013) Role of p38 and JNK MAPK signaling pathways and tumor suppressor p53 on induction of apoptosis in response to AdeIF5A1 in A549 lung cancer cells. Mol Cancer 12:35–45. doi:10.1186/1476-4598-12-35
21. Wilhelm C, Billotey C, Roger J, Pons JN, Bacri JC, Gazeau F (2003) Intracellular uptake of anionic superparamagnetic nanoparticles as a function of their surface coating. Biomaterials 24:1001–1011. doi:10.1016/S0142-9612(02)00440-4
22. Patil S, Sandberg A, Heckert E, Self W, Seal S (2007) Protein adsorption and cellular uptake of cerium oxide nanoparticles as a function of zeta potential. Biomaterials 28:4600–4607. doi:10.1016/j.biomaterials.2007.07.029
23. Lim HK, Asharani PV, Hande MP (2012) Enhanced genotoxicity of silver nanoparticles in DNA repair deficient Mammalian cells. Front Genet 3:104–116. doi:10.3389/fgene.2012.00104
24. Derfus AM, Chan WCW, Bhatia SN (2004) Intracellular delivery of quantum dots for live cell labeling and organelle tracking. Adv Mater 16:961–966. doi:10.1021/nl102172j
25. Xia T, Kovochich M, Brant J, Hotze M, Sempf J, Oberley T, Sioutas C, Yeh JI, Wiesner MR, Nel AE (2006) Comparison of the abilities of ambient and manufactured nanoparticles to induce cellular toxicity according to an oxidative stress paradigm. Nano Lett 6:1794–1807. doi:10.1021/nl061025k
26. Zhivotovsky B, Orrenius S, Brustugus OT, Doskeland SO (1998) Injected cytochrome c induces apoptosis. Nature 391:449–50. doi:10.1038/35060
27. Johnson BW, Cepero E, Boise LH (2000) Bcl-xL inhibits cytochrome c release but not mitochondrial depolarization during the activation of multiple death pathways by tumor necrosis factor-alpha. J Biol Chem 275:31546–31553. doi:10.1074/jbc.M001363200
28. Piao MJ, Kang KA, Lee IK, Kim HS, Kim S, Choi JY, Choi J, Hyun JW (2011) Silver nanoparticles induce oxidative cell damage in human liver cells through inhibition of reduced glutathione and induction of mitochondria-involved apoptosis. Toxicol Lett 201:92–100. doi:10.1016/j.toxlet.2010.12.010
29. Cargnello M, Roux PP (2011) Activation and function of the MAPKs and their substrates, the MAPK-activated protein kinases. Microbiol Mol Biol Rev 75:50–83. doi:10.1128/MMBR.00031-10
30. Hsin YH, Chen CF, Huang S, Shih TS, Lai PS, Chueh PJ (2008) The apoptotic effect of nanosilver is mediated by a ROS and JNK dependent mechanism involving the mitochondrial pathway in NIH3T3 cells. Toxicol Lett 179:130–139. doi:10.1016/j.toxlet.2008.04.015